

PDMS Based Thermopneumatic Microvalve for Microfluidic Systems

Suriya Mongpraneet^{a,b,*}, Thoatsanope Kamnerdtong^a, Pattaramon Jongpardist^a
Anurat Wisitsora-at^b and Adison Tuantranont^b

^aDepartment of Mechanical Engineering, Faculty of Engineering, King Mongkut's University of Technology, Thonburi, Bangmod, Toongkru, Bangkok 10140

^bNanoelectronics and MEMS Laboratory, National Electronics and Computer Technology Center (NECTEC), Klong1, Klong Luang, Pathumthani 12120

*E-mail: suriya.mongpraneet@nectec.or.th

Abstract

A thermopneumatic microvalve for switching fluid in a microchannel of PDMS based microfluidic chip was designed and fabricated from multi-stack PDMS structure on a glass substrate. Microvalve structure consists of inlet and outlet, microchannel, a thermopneumatic actuation chamber, and a thin film heater. In microchannel, fluid is blocked or passed by the motion of actuation diaphragm. Actuation diaphragm is bent up and down by exploiting air expansion that is induced by increasing heater temperature. The microvalve was designed and simulated by CoventorWareTM, MEMS commercial finite element simulation software, to predict its characteristics and optimize the design. The microvalve created for simulation model has a diameter of 2.5 mm and a total height of 450 μm . The microvalve was then fabricated on glass substrate by low cost processes including PDMS spinning, oxygen plasma bonding, electroplated micromasking, and thermal evaporation. The microvalve characteristics were measured as a function of applied voltage and inlet pressure. From the experiment, a maximum inlet pressure of 10 kPa can be applied with 7 - 17 V applied voltage to the microvalve heater. The leak rate and maximum inlet pressure results obtained from CoventorWareTM agree well with the experimental data.

Keywords: actuation, bonding, electroplated

1. Introduction

In recent years, microvalves are often one of the most important components for the realization of a full integrated microfluidic system, such as lab-on-a-chip or micro total analysis system (μTAS). Thermopneumatic microvalves are performed by volumetric thermal expansion couple to diaphragm deflection. Typically, has an actuator with a sealed chamber and movable diaphragm, where the gas phase system is heated by resistor (microheater) incorporated in the chamber [1-2].

The polydimethylsiloxane (PDMS) with low Young's modulus and high reversible strain allows for large stroke and high sealing performance, as well as effective adherence between glasses in the structure. A chamber and microchannels can be made in a cross-

configuration separated by a thin film of PDMS. Applying pressure in the chamber, the PDMS film is deformed so that in the cross-section of the adjacent channel is changed, resulting an effective actuation [3]. Similarly, advanced microfluidic devices can then be fabricated for chemical and biological applications [4-5]. The microvalve consists of three main components including microchannel, actuation diaphragm attached to actuation chambers, and heaters on glass slide. The cross-sectional view of microvalve is depicted in Fig 1 to demonstrate the operating principle of the peristaltic microvalve. Initially, each of heaters is supplied with driving voltage to its corresponding electrical pad. The temperature of heater is increased by Joule's heating effect causing the air inside actuation chamber to expand and the flexible actuation diaphragm to move up to microchannel [6]

In this work, we study the response of the PDMS microvalves by finite element method and measure the temperature of a microheater through the microvalve section that is controlled pneumatically. By systematically changing the voltage applied to microheater in the chamber, the optimal condition for actuation in several types of microfluidic components can be determined.

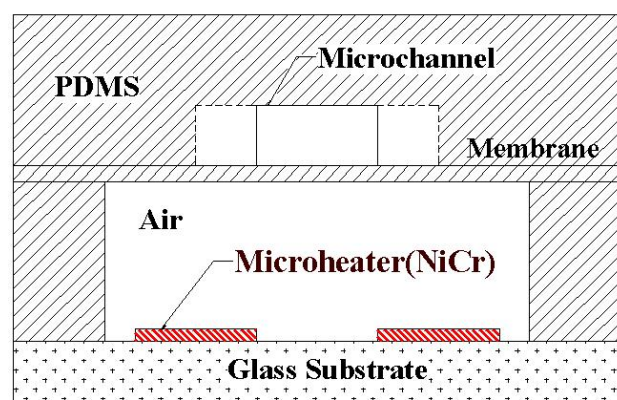


Fig. 1 Cross-section view of thermopneumatic microvalve.

2. Fabrication process

The process diagram for thermo-pneumatic microvalve fabrication is shown in Fig. 2 (a) and (b). The process consists of two main parts, sputtering of nichrome microheater and molding PDMS microchannel. In the first part, the substrate for electroplating is a 2 mm-thick stainless steel plate. First, a 38 μm -thick dry photoresist film was laminated on a cleaned stainless steel plate by a commercial rolling-laminating machine at 80 $^{\circ}\text{C}$. It should be noted that dry photoresist film is chosen instead of wet photoresist because of its suitable thickness. Conventional photolithography was then performed to obtain desired patterns of photoresist on the substrate. In the photolithography process, the photoresist-coated plate was exposed under 360 nm ultraviolet (UV) light from a 300 W UV source for 3 seconds. The photo mask was a thin sheet of dark film patterned by a commercial pattern generator system. The pattern was microheater that consisted of 300 μm wide microheater. After exposure, the photoresist was developed for 90-120 seconds. Next, the patterned substrate was surface-treated by immersion in 20%-potassium-dichromate ($\text{K}_2\text{Cr}_2\text{O}_7$) aqueous solution for 5 minutes to form a very thin layer of chromium oxide on the stainless steel surface. It was necessary to form the oxide to facilitate detachment of electroplated Ni structure from the stainless steel substrate. Ni-electroplating process was then performed on the substrate. In electroplating process, the substrate (cathode) was biased at a negative potential relative to counter electrode in nickel sulphate plating solution. The electroplating was conducted at constant current varying from 0.1 to 0.4 A/dm^2 for 4 hours. The electroplated Ni microstructures were detached from the substrate by simple peeling off method. The thickness of the plated structure was measured to be 43 μm by a white-light interferometer (Polytech Inc.). The photograph of nickel-electroplated microshadow mask is shown in Fig. 3 (a).

Finally, the micro-electroplated structure is then used as templates for pattern transfer on glass substrates via sputtering through shadow masking. The shadow mask was put in front of glass substrate (1 mm-thick) and strong magnets were then placed behind to attract the micro-electroplated Ni templates to the substrates. The magnet is very important for pattern transfer from microelectroplated structures because the transfer of micron-scale patterns requires an intimate contact between the substrates and the mask templates. The assembled structures were then loaded into a magnetron sputtering system. After a base vacuum environment of 3×10^{-6} mbar, the substrates were cleaned by RF plasma at an argon pressure of 3×10^{-3} mbar. This cleaning was to improve adhesion of the film to the substrates by removing moisture and any organic contaminants on the surface. The 50 nm thick chromium film was then deposited by DC sputtering at room temperature under an argon pressure of 3×10^{-3} mbar. This thin Cr layer was used as an adhesive layer for subsequent nichrome (Ni 80% Cr 20%) film on glass substrate. 0.5 μm thick

Nichrome layer was sputtered on the Cr layer. Typical photograph of nichrome patterns on glass substrates is shown in Fig. 3 (b).

The second part starts from mold fabrication using SU-8 negative photoresist (MicroChem co.,ltd). Before spin coating, a 500 μm -thick 3 inch silicon substrate was ground and precleaned by oxygen plasma treatment at 35 W RF power for 10 minutes. The SU-8 No. 2100 photoresist was then pre-spun at 500 rpm for 5 seconds and then spun at speed of 3000 rpm for 30 seconds. Next, SU-8 film was pre-baked on a hot plate at 60 $^{\circ}\text{C}$ for 5 minutes at each temperature and then soft-baked at 95 $^{\circ}\text{C}$ for 60 minutes before slowly cooling down to room temperature. In the photolithography process, the photoresist-coated plate was exposed under 360 nm ultraviolet (UV) light from a 300 W UV source for 10 seconds. The photo mask was a thin sheet of dark film patterned by a commercial pattern generator system. The pattern was a 200 μm wide microchannel. After exposure, the photoresist was developed for 90-120 seconds. The photograph of the SU-8 mold on silicon wafer for PDMS microchannel casting is shown in Fig. 4. Then, 10:1 of PDMS (Dow Corning Sylgard 184) base and curing agent were mixed and degassed for filling up SU-8 mold. PDMS microchannel replica is peeled off from mold and inlet/outlet ports are made by hole-punching. Fig. 5 shows the photographs of the microheater on glass substrate and microchannel before final bonding process.

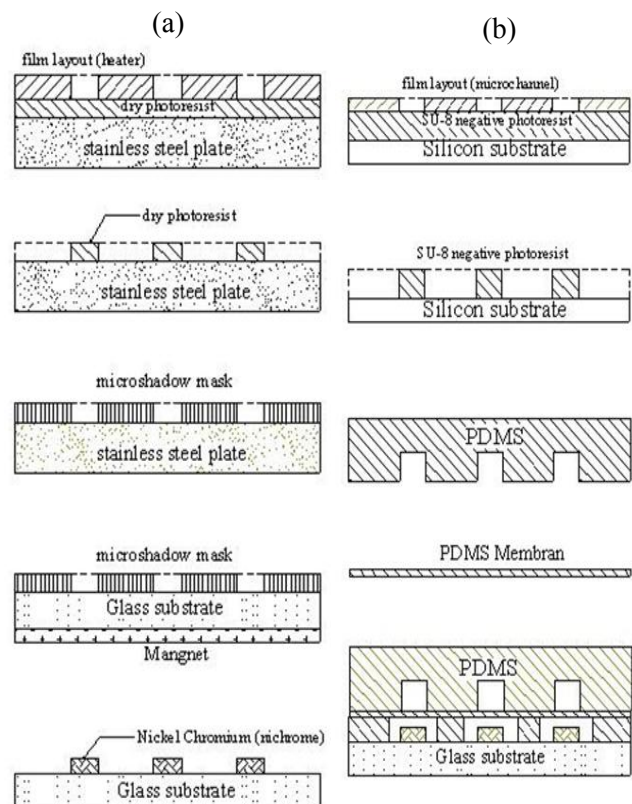


Fig. 2 Schematic presentation the thermo-pneumatic valve fabrication (a) the process diagram for microheater and (b) the process diagram for microchannel.

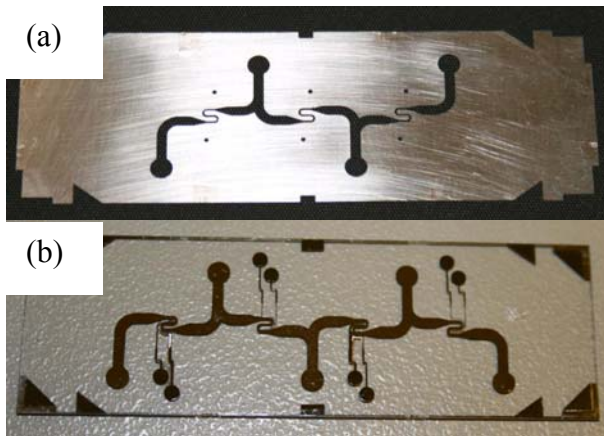


Fig. 3 Photograph of (a) electroplated Ni microshadow mask and (b) nichrome patterns on glass substrates.

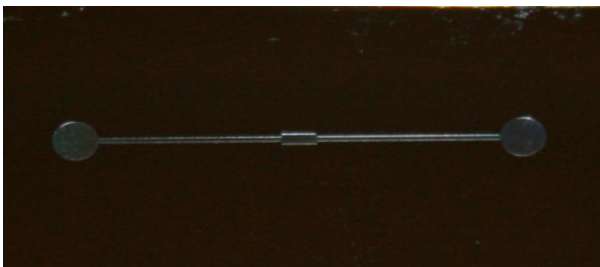


Fig. 4 Photographs of SU-8 mold on silicon wafer.

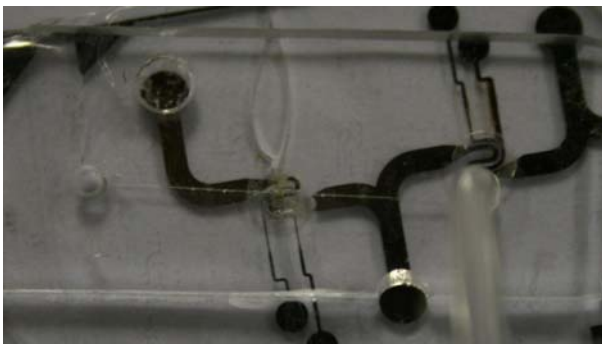


Fig. 5 Photographs of the microheater on glass substrate and microchannel before final bonding process

3. Experiment and Simulation

3.1 Microheater

The characteristic of microheater is characterized by varying applied voltage and measuring its temperature by a commercial temperature sensor. The characteristic of temperature sensor as a function of time and voltage is shown in Fig. 6. The measured temperature should be lower than the true temperature of the microheater because loading effect of temperature sensor, which is very large of compared to the microheater.

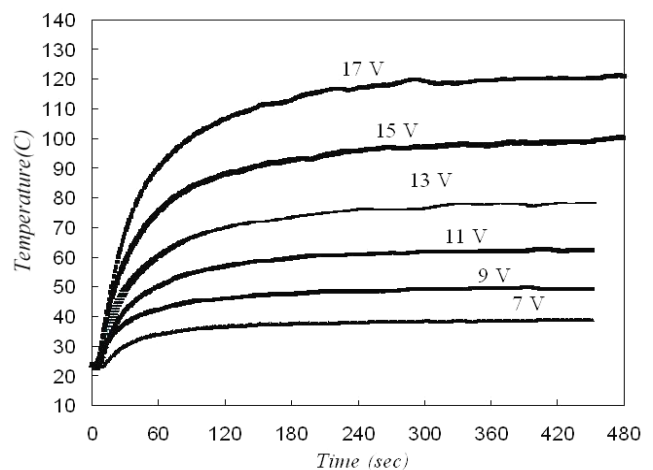


Fig. 6 Characteristic of temperature sensor as a function of time and voltage.

3.2 PDMS microvalve

Multi-layer soft lithography has been used for the rapid prototyping of Microvalve as conceptually illustrated in Fig. 1. It consists of a three layer PDMS microchannel structure bonded on a glass substrate. Both the flow and control channels are designed to have an initial channel width of 200 μm and a height of 100 μm . The microvalve was tested using air as a working fluid instead of DI water for simplicity in experiment. Fig. 6 illustrates the experimental setup for microvalve testing. Voltage is supplied to the microvalve to control water flow, which is pumped by a syringe pump through the regulator and mass flow meter.

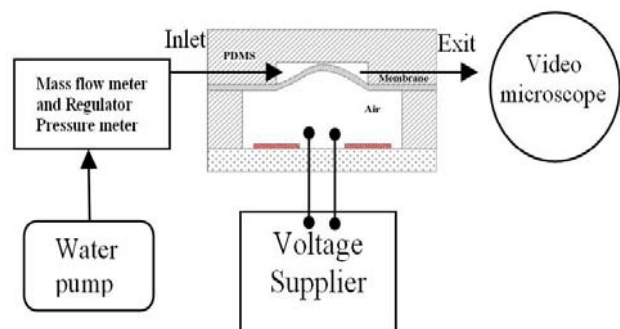


Fig. 6 The experiment setup for microvalve testing.

3.3 Displacement Simulation

The temperature of heater is increased by Joule's heating effect causing the air inside actuation chamber to expand and the flexible actuation diaphragm to move up to microchannel. The air pressure in the actuation chambers can be estimated from ideal gas law:

$$p = \rho RT \quad (1)$$

where ρ is density, p is pressure, R is the gas constant, and T is temperature.

Table 1. Material property

Material	Glass	Nichrome	Air	PDMS
Young's modulus (MPa)	4.00e+07	2.28e+5	-	5.00e-01
Possion Ratio	1.70e-01	3.05e-1	-	6.15e-01
Density (kg/ μ m ³)	2.23e-15	6.33e-15	1.16e-18	9.08e-16
Specific Heat (pJ/kg.K)	8.35e+14	4.44e+14	1.01e+15	1.01e+15
Electrical Conductivity (pS/ μ m)	-	2.16e-15	-	-
Thermal Conductivity (pW/ μ m.K)	1.40e+06	9.05e+07	2.62e+04	2.62e+00

The simulated model was a 5.0 mm wide, 5.0 mm long, and 0.45 mm high microvalves. The 3D model was meshed with suitable hexagonal mesh with the number of element \approx 30000 and type of element C3D20R as shown in Fig. 7. The structure was then simulated by CoventorWare™ static using general module. In addition, the simulations are performed with different pressures of 20.45 kPa, 29.94 kPa, 42.07 kPa, 59.37 kPa, and 81.76 kPa, respectively.

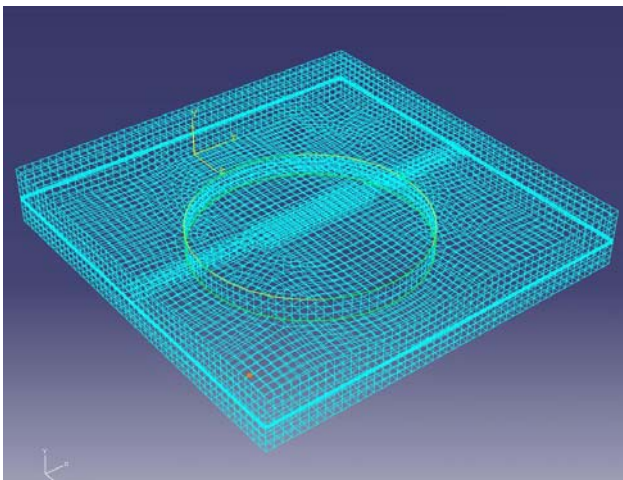


Fig. 7 3D model of simulated diaphragm in microvalve with hexagonal mesh.

Table 2. Relationship of voltages, temperature and pressures

V(V)	T (°K)	P (kPa)
7	339.62	14.2
9	357.99	20.45
11	385.87	29.94
13	421.53	42.07
15	472.37	59.37
17	538.18	81.76

4. Results and Discussions

The deformation of diaphragm simulation yields air pressures applied on the chamber structure. Typical 3D temperature profile in the microvalve structure is shown in Fig. 8. Fig. 9 shows 3D cross-section of microvalve demonstrating diaphragm moving up to microchannel.

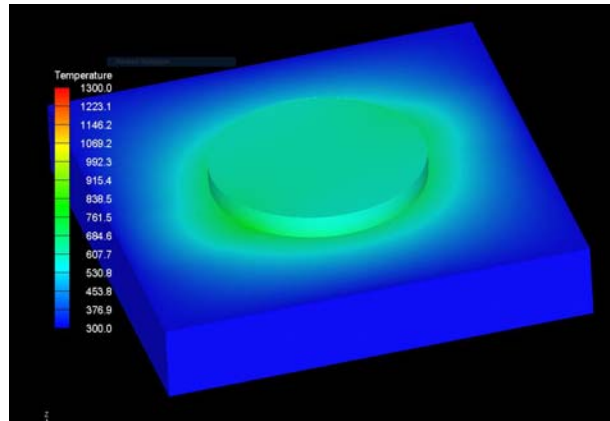


Fig. 8 3D simulated result of air temperature in chamber from thermopneumatic microvalves.

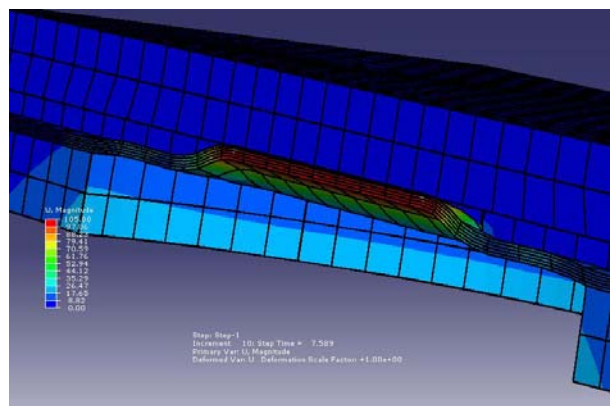


Fig. 9 3D cross-section of microvalve demonstrating diaphragm moving up to microchannel.

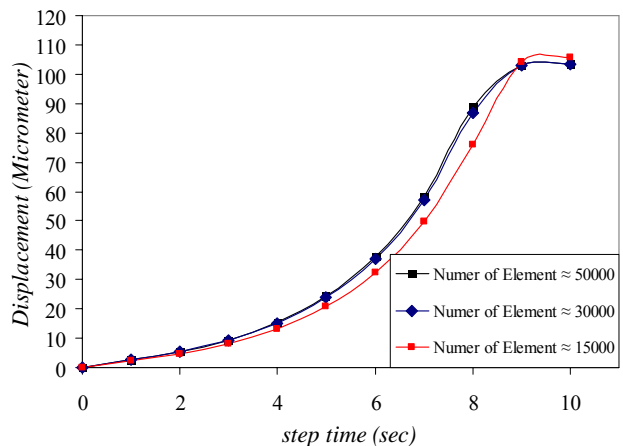


Fig. 10 Displacements of actuation diaphragm vs. time plots simulated with different number of elements.

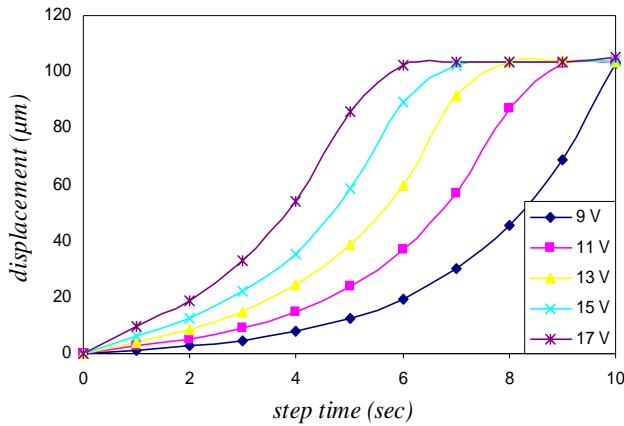


Fig. 11 Displacements of actuation diaphragm vs. time plots for different applied voltages.

Fig. 10 shows displacements of actuation diaphragm vs. time plots simulated with different number of elements. It can be seen that the number of elements of 30,000 provide sufficient accuracy. Fig. 11 shows displacements of actuation diaphragm vs. time plots for different applied voltages. It can be seen that the displacement is increased with higher rate as the applied voltage increased, however, displacements of actuation diaphragm has slow responsibility and motion toward microchannel because the big chamber with values of specific heat and thermal conductivity less compare with other working fluid.

5. Conclusion

In this paper, a thermopneumatic microvalve has been designed and fabricated. The microvalve is constructed using a simple fabrication process that allows it to be integrated with other plastic based microfluidic devices and circuits. The deformation behaviors of diaphragm in the microvalve have been evaluated by finite element simulation using CoventorWare™ program. Displacement of diaphragm move up to microchannel is faster as the applied voltage to microrheater increases.

References

1. C. Zhang, D. Xing, 2007. Micropump, microvalve and micromixers with in PCR microfluidic chips: Advances trends. *Biotechnology Advances*, Vol. 25, pp.483-514
2. T. Otori, S. Shoji, 1998. Partly disposable three-way microvalve for a medical micro total analysis system (μ TAS). *sensors and Actuators*, Vol. 64, pp.57-62
3. J.-C. Galas, V. Studer, 2005. Characterization of pneumatically activated microvalves by measuring electrical conductance. *Microelectronic Engineering* Vol.78–79, pp.112–117
4. J. Peter, S. Gemmem, 2007. Effects of cell-to-cell fuel mal-distribution on fuel performance and a mean to reduce mal-distribution using MEMS micro-valve. *Power Sources*. Vol. 164, pp.115-125

5. Teruo Fuji, 2002 . PDMS–base microchannel devices for biomedical application. *Microelectronic Engineering* Vol.61–62, pp.907–914
6. A. Tuantranont, A. Wisitsoraat, 2007. PDMS Based Thermopneumatic Peristaltic Micropump for Microfluidic Systems.